QIAO, J., WANG, S., YU, C., YANG, X. and FERNANDEZ, C. 2022. A novel intelligent weight decreasing firefly-particle filtering method for accurate state-of-charge estimation of lithium-ion batteries. *International journal of energy research* [online], 46(5), pages 6613-6622. Available from: https://doi.org/10.1002/er.7596

# A novel intelligent weight decreasing firefly-particle filtering method for accurate state-of-charge estimation of lithium-ion batteries.

QIAO, J., WANG, S., YU, C., YANG, X. and FERNANDEZ, C.

2022

INTERNATIONAL JOURNAL OF
ENERGY RESEARCH

# A novel intelligent weight decreasing firefly - particle filtering method for accurate state-of-charge estimation of lithium-ion batteries

| | |
|---|---|
| Journal: | *International Journal of Energy Research* |
| Manuscript ID | ER-21-22214.R1 |
| Wiley - Manuscript type: | Research Article |
| Date Submitted by the Author: | 13-Dec-2021 |
| Complete List of Authors: | Qiao, Jialu; Southwest University of Science and Technology,<br>Wang, Shunli; Southwest University of Science and Technology, School of Information Engineering<br>Yu, Chun-Mei; Southwest University of Science and Technology, School of information engineering<br>Yang, Xiao<br>Fernandez, Carlos; Robert Gordon University |
| Keywords: | lithium-ion battery, second-order RC equivalent circuit model, state-of-charge, intelligent weight decreasing firefly, particle filtering |
| | |

# A novel intelligent weight decreasing firefly - particle filtering method for accurate state-of-charge estimation of lithium-ion batteries

**Jialu Qiao[a], Shunli Wang[a*], Chunmei Yu[a], Xiao Yang[a], Carlos Fernandez[b]**

*[a]School of Information Engineering, Southwest University of Science and Technology, Mianyang 621010, China; [b]School of Pharmacy and Life Sciences, Robert Gordon University, Aberdeen AB10-7GJ, UK.*

**Abstract:** Accurate state-of-charge estimation plays an extremely crucial role in battery management systems. To realize the real-time and precise state-of-charge estimation, an intelligent weight decreasing firefly - particle filtering algorithm is proposed. In this research, the second-order RC equivalent circuit model is established and the parameters are identified online, state-of-charge particles simulate the attraction behavior of fireflies in nature and approach the global optimal value to complete the particle optimization process. The linear weight decreasing strategy is introduced to avoid the algorithm falling into local optimization. The data of different complex conditions are used to verify the feasibility of the proposed algorithm, the results show that the root-mean-square error of intelligent weight decreasing firefly - particle filtering method when the initial SOC value is set to 1 under Hybrid Pulse Power Characterization and Beijing Bus Dynamic Stress Test condition can be controlled within 0.60% and 1.12% respectively, which verifies that the proposed algorithm has high accuracy in state-of-charge estimation of lithium-ion batteries. The algorithm proposed in this paper provides a theoretical basis for real-time state monitoring and security of battery management systems.

**Key words:** lithium-ion battery; second-order RC equivalent circuit model; state-of-charge; intelligent weight decreasing firefly; particle filtering

## 1. Introduction

In recent years, many countries have begun to change the energy supply structure and vigorously develop new energy to alleviate the energy crisis and environmental pollution [1,2]. The continuous development and utilization of new energy and its energy storage devices have laid a foundation for the development of electric vehicles [3]. Guided by energy conservation and emission reduction, the automotive industry began to transform, and electric vehicles have become the main direction of its development [4]. The overcharge and over discharge of lithium-ion batteries in the use of electric vehicle need to be solved urgently [5], which will not only lead to serious battery heating, but also damage the battery life, and even lead to thermal runaway of battery, resulting in personal safety and property loss [6, 7]. In addition, mileage anxiety is also an important problem in the use of electric vehicles [8]. Therefore, a stable and reliable battery management system (BMS) must be adopted in the use of lithium-ion batteries to ensure the safe and stable operation, monitor the service status and make efficient use of the discharge performance of lithium-ion batteries [9, 10]. State-of-charge (SOC) is a key parameter in BMS, it is equivalent to the fuel gauge of vehicles [11], providing the driver with real-time status of the vehicle and a better driving experience [12], and it also provides the basis for the calculation of other state parameters of electric vehicles [13]. As the key and difficult point of electric vehicle development [14,15], SOC estimation has important research significance.

Accurate battery modeling is of great significance to SOC estimation [16]. There are complex electrochemical reactions in lithium-ion batteries under random discharge conditions [17,18]. Battery model is often used to describe the behavior of battery under external excitation [19]. There are three kinds of commonly used lithium-ion battery models: electrochemical model, data-driven model and equivalent circuit model [20]. Electrochemical model is often used to describe the electrochemical reaction process inside the battery [21], which can deeply reflect the complex electrochemical kinetic mechanism [22]. However, it is too complex, large amount of calculation and difficult to solve online [23]. The data-driven model relies on a large number of test data to establish the relationship between input and output [24], without considering the complex electrochemical reaction process inside the battery [25], but a large number of tests need to spend a long time and cost [26]. The equivalent circuit model makes a balance between model accuracy and real-time calculation, which opens up a way for online SOC estimation [27]. The circuit network structure composed of common circuit elements is used to describe the external characteristics of the battery. At present, it is the most widely used model in the process of SOC online estimation [28].

Researchers introduced fading factor into traditional extended Kalman filter (EKF) algorithm to improve the estimation accuracy, which solves the problem of easy divergence in the later stage of EKF to a certain extent [29]. Aiming at the problem of large error caused by inaccurate initial value when Ampere-hour (Ah) algorithm estimates SOC of lithium-ion batteries, an algorithm combining improved particle filter (PF) and Ah is proposed in [30], the fused algorithm has higher accuracy and response speed. With the rise of population intelligent stochastic optimization algorithms in recent years, aiming at the problem of particle dilution in traditional PF, an improved bat algorithm is proposed to optimize PF to estimate SOC in [31]. The particle is represented as a bat individual, the predation process of bat population is simulated, and the particle dilution problem is solved, which obtains good accuracy.

To precisely describe the working state of the lithium-ion batteries, a firefly algorithm of population intelligence random optimization is combined with PF algorithm. By treating particles as fireflies, their attraction behavior in nature is simulated, and then the optimization of particles is explored. The linear weight decreasing strategy is introduced to avoid the algorithm falling into local optimization. The proposed novel algorithm is named intelligent weight decreasing firefly - particle filtering (IWDF - PF) method. Combined with the establishment of second-order RC equivalent model and online parameter identification, the proposed algorithm is verified by experiments under two complex working conditions.

## 2. Mathematical analysis

To obtain the current SOC of the batteries precisely, it is essential to establish an appropriate battery model. Proper model selection and accurate parameter identification are the foundation of SOC estimation.

### *2.1. Second-order RC equivalent circuit modeling*

The equivalent circuit model uses common circuit elements, such as resistance, capacitance, voltage source and so on, to form a circuit network structure to describe the external characteristics of the battery. The influence of battery polarization factor is added based on Rint model to form the Thevenin model, which can overcome the error caused by polarization effect. Based on it, a group of RC circuits is added to form a second-order RC equivalent model, which can more accurately characterize the dynamic characteristics of the battery and has an appropriate calculation work. The parallel RC network represents the polarization process of the battery, the number of RC circuits is too small to precisely describe the behavior characteristics of the battery. Too many RC circuits will increase the difficulty of online parameter identification and can not significantly increase the accuracy of the model. To better balance the model accuracy and real-time calculation, the second-order RC equivalent circuit model is established, which is shown in Fig. 1.

In Fig. 1, the open circuit voltage is represented by $U_{OC}$, the terminal voltage is represented by $U_L$, the ohmic internal resistance is represented by $R_0$. The first RC parallel circuit is composed of electrochemical polarization resistance $R_1$ and electrochemical polarization capacitance $C_1$. The second RC parallel circuit is composed of concentration polarization resistance $R_2$ and concentration polarization capacitance $C_2$. $R_1C_1$ loop represents the process of rapid change of circuit voltage, and $R_2C_2$ loop represents the process of slow change of circuit voltage. With the discharge direction as positive, the KVL equation of the circuit is listed as shown in Eq. (1).

$$\begin{cases} U_L = U_{OC} - I(t)R_0 - U_1 - U_2 \\ \dfrac{dU_1}{dt} = -\dfrac{U_1}{R_1C_1} + \dfrac{I}{C_1} \\ \dfrac{dU_2}{dt} = -\dfrac{U_2}{R_2C_2} + \dfrac{I}{C_2} \end{cases} \tag{1}$$

Where, $[\mathrm{SOC}\ U_1\ U_2]^T$ is selected as the state variable. By discretizing the equivalent circuit, the state space expression of the model can be obtained as shown in Eq. (2).

$$\begin{cases} \begin{bmatrix} SOC_{k+1} \\ U_{1,k+1} \\ U_{2,k+1} \end{bmatrix} = \begin{bmatrix} 1 & 0 & 0 \\ 0 & e^{-\Delta t/\tau_1} & 0 \\ 0 & 0 & e^{-\Delta t/\tau_2} \end{bmatrix} \begin{bmatrix} SOC_k \\ U_{1,k} \\ U_{2,k} \end{bmatrix} + \begin{bmatrix} -\dfrac{\Delta t}{Q_N} \\ R_1\left(1-e^{-T/\tau_1}\right) \\ R_2\left(1-e^{-T/\tau_2}\right) \end{bmatrix} I_k + w_k \\ U_{L,k+1} = U_{OC,k+1} - U_{1,k+1} - U_{2,k+1} - IR_0 + v_k \end{cases} \tag{2}$$

Eq. (2) shows the state equation and observation equation of the system respectively. $\Delta T$ is the sampling time, $\tau$ is the time constant, $\tau_1=R_1C_1$, $\tau_2=R_2C_2$. $w_k$ represents process noise and $v_k$ represents observation noise. $Q_N$ is the rated capacity of the battery. $k$ represents the current time point, and $k + 1$ represents the next time point.

### *2.2. High precision online parameter identification*

Recursive least square (RLS) method is a recursive algorithm derived from the least square method, which is the most frequently used method for battery model parameter identification. The memory length of RLS is infinite, with the increase of recurrence times, the proportion of old data will gradually increase, making it difficult for new data to correct, resulting in the weakening of estimation effect and worse estimation effect in time-varying systems. To avoid the above situation, the recursive least square with forgetting factor (FFRLS) is used for parameter identification. The forgetting factor is added to the RLS, which can reduce the occupation of old data in matrix $P$ ($k$), to prevent data saturation and obtain more accurate identification results. The FFRLS recursive equations are shown as Eq. (3).

$$\begin{cases} \theta_{k+1} = \theta_k + K_{k+1}\left[y(k+1) - h(k+1)\theta_k\right] \\ P_{k+1} = \left[P_k - K_k h^T(k+1)P_k\right]\lambda^{-1} \\ K_{k+1} = P_k h(k+1)\left[\lambda + h^T(k+1)P_k h(k+1)\right]^{-1} \end{cases} \tag{3}$$

In Eq. (3), $\theta$ ($k$) is the parameter matrix to be identified of the system at time $k$, $P$ ($k$) is the covariance matrix of the algorithm at time $k$, $K$ ($k$) is the gain matrix at time $k$, $\lambda$ is the forgetting factor introduced and the value is 0.95. The equivalent circuit model is rewritten into the form of discrete-time series, as shown in Eq. (4).

$$U_{OC} = U_L + \left(\frac{R_1}{R_1C_1s+1} + \frac{R_2}{R_2C_2s+1} + R_0\right)I \tag{4}$$

Let the time constant $\tau_1 = R_1C_1$, $\tau_2 = R_2C_2$, and $a = \tau_1\tau_2$, $b = \tau_1+\tau_2$, $c = R_0+R_1+R_2$, $d = R_1\tau_2+R_2\tau_1+R_0(\tau_1+\tau_2)$, Eq. (4) can be rewritten as Eq. (5).

$$aU_{OC}s^2 + bU_{OC}s + U_{OC} = aR_0I_s^2 + dI_s + cI + aU_s^2 + bU_s + U_L \tag{5}$$

Substitute $s = [x(k)\text{-}x(k\text{-}1)]/T$ into Eq. (5) for discretization, where $T$ is the sampling time, as shown in Eq. (6).

$$\begin{cases} U_{OC}(k) - U_L(k) = \dfrac{-bT-2a}{T^2+bT+a}\left[U_L(k-1) - U_{OC}(k-1)\right] + \dfrac{a}{T^2+bT+a}\left[U_L(k-2) - U_{OC}(k-2)\right] \\ + \dfrac{cT^2+dT+aR_0}{T^2+bT+a}I(k) + \dfrac{-dT-2aR_0}{T^2+bT+a}I(k-1) + \dfrac{aR_0}{T^2+bT+a}I(k-2) \end{cases} \tag{6}$$

The parameters are abstracted and replaced by [$k_1$, $k_2$, $k_3$, $k_4$, $k_5$] as shown in Eq. (7).

$$\begin{cases} U_{OC}(k)-U_L(k)=k_1\left[U_L(k-1)-U_{OC}(k-1)\right]+k_2\left[U_L(k-2)-U_{OC}(k-2)\right] \\ +k_3 I(k)+k_4 I(k-1)+k_5 I(k-2) \end{cases} \tag{7}$$

The values of [$k_1$, $k_2$, $k_3$, $k_4$, $k_5$] are shown in Eq. (8).

$$\begin{cases} k_1=\dfrac{-bT-2a}{T^2+bT+a}, k_2=\dfrac{a}{T^2+bT+a}, \\ k_3=\dfrac{cT^2+dT+aR_0}{T^2+bT+a}, k_4=\dfrac{-dT-2aR_0}{T^2+bT+a}, k_5=\dfrac{aR_0}{T^2+bT+a} \end{cases} \tag{8}$$

Eq. (7) can be substituted into the FFRLS, the identification parameter vector is $\theta = (k_1, k_2, k_3, k_4, k_5)^T$. After deriving the parameter identification results, the actual parameters of the battery can be obtained by parameter separation as shown in Eq. (9).

$$\begin{cases} R_0=\dfrac{k_5}{k_2} \\ R_1=(\tau_1 c+\tau_2 R_0-d)/(\tau_1-\tau_2) \\ R_2=c-R_1-R_0 \\ C_1=\tau_1/R_1, C_2=\tau_2/R_2 \end{cases} \tag{9}$$

*2.3. Intelligent weight decreasing firefly - particle filtering*

Compared with the traditional linear filtering algorithm, PF is appropriate for nonlinear and non-Gaussian noise environments and has better nonlinear state estimation performance. PF is a typical Bayesian filtering recursive process, which mainly includes five steps: particle initialization, updating particle state and weight, weight normalization, resampling and predicting particle state. The algorithm flow chart is shown in Fig. 2.

The biggest drawback of the traditional PF algorithm is that its resampling method reduces particle degradation and scarcity by eliminating a group of particles with a small weight, but the particle diversity will be reduced after multiple resampling, so it is necessary to optimize it. Firefly algorithm is innovatively introduced to solve this problem.

Firefly algorithm is a population intelligent random optimization algorithm, which is realized by simulating the population behavior of fireflies in nature. In this algorithm, the firefly is regarded as an independent signal unit to attract other fireflies around by emitting fluorescence. The basic assumptions of the algorithm are as follows:

First, any firefly in a given space will be attracted to fireflies with a higher brightness than itself, and will not be affected by individual differences. Second, the degree of attraction of fireflies is directly proportional to the brightness of their fluorescence. Third, if a given firefly in space fails to find someone brighter than itself, the firefly will move randomly. The relative fluorescence brightness of fireflies is calculated as shown in Eq. (10).

$$I = I_0 \times e^{-\gamma \times r_{ij}} \tag{10}$$

In Eq. (10), $I$ is the relative fluorescence brightness and $I_0$ is the maximum fluorescence brightness. The higher the self-fluorescence brightness of the firefly, the better the corresponding objective function value. The spatial distance between firefly $i$ and $j$ is expressed as $r_{ij}$; $\gamma$ is the absorption coefficient of the medium to the fluorescence intensity. The attraction of fireflies is calculated as shown in Eq. (11).

$$\beta = \beta_0 \times e^{-\gamma \times r_{ij}{}^2} \tag{11}$$

In Eq. (11), $\beta$ is the attraction between fireflies, and $\beta_0$ is the maximum attraction of fireflies. The location update of fireflies is shown in Eq. (12).

$$x_i = x_i + \beta \times (x_j - x_i) + \alpha \times (rand - 0.5) \tag{12}$$

In Eq. (12), $x_i$, $x_j$ is the spatial position of fireflies $i$ and $j$; $\alpha$ is the step factor, with a value of 0.2; *rand* is a random number that obeys uniform distribution on [0,1].

In PF algorithm, the difference between the particle and the optimal value is regarded as the relative fluorescence brightness of the particle. Therefore, this study introduces the estimation results into the adaptive iterative optimization of firefly algorithm to ensure the accuracy of the filter. The modified fluorescence brightness calculation equation is adopted as shown in Eq. (13).

$$I = \left[SOC_{opt} - SOC_{pred}(i)\right]^2 \tag{13}$$

To enhance the convergence speed and precision of firefly algorithm, this research introduces the linear decreasing strategy of weight into the standard firefly algorithm. The adjusted equation is shown in Eq. (14).

$$\omega_k = \omega_{\max} - \frac{\omega_{\max} - \omega_{\min}}{iter_{\max}} \times iter \tag{14}$$

In Eq. (14), *iter* and $iter_{max}$ are expressed as the current number of iterations and the maximum number of iterations, $\omega_k$ represents the current weight value, $\omega_{\max}$, $\omega_{\min}$ is the maximum and minimum value of weight respectively. Accordingly, the position update equation is modified as shown in Eq. (15).

$$x_i = \omega_k \times x_i + \beta \times (gbest - x_i) + \alpha \times (rand - 0.5) \tag{15}$$

Where *gbest* is the global optimal value in one iteration. In this study, the weight decreasing firefly algorithm is combined with the traditional PF algorithm to optimize it. The complete process of the proposed novel IWDF - PF method is shown in Fig. 3.

## 3. Experimental analysis

To test the feasibility of the novel IWDF - PF method, two complex working conditions of HPPC (Hybrid Pulse Power Characterization) and BBDST (Beijing Bus Dynamic Stress Test) are selected for experimental verification. The online parameter identification is carried out under these two tests, the identification results are used for SOC estimation, and the IWDF - PF algorithm is compared with the traditional PF for more convincing verification.

### *3.1. Construction of experimental platform*

Lithium-ion battery cell with a rated capacity of 45AH is used for experimental equipment, BTS750-200-100-4 battery testing equipment is used as the test platform of this research. Because the characteristics of the battery will be affected by temperature, the experiments in this research are carried out at room temperature of 25 ℃.

### *3.2. Online parameter identification results*

The experimental data of HPPC working condition are used for online battery parameter identification. The whole process of HPPC experiment is shown in Fig. 4.

Open circuit voltage (OCV) can only be measured accurately when the battery reaches a stable state. By obtaining the voltage data of the shelved part in the HPPC experiment, the OCV corresponding to SOC from 0.1, 0.2 to 1 is obtained, and the SOC-OCV function relationship is obtained by curve fitting. The function relationship is applied to FFRLS to obtain the parameter identification results of the experimental battery under HPPC operating condition, the dynamic changes of battery internal parameters with SOC obtained by online identification are shown in Fig. 5.

The variation of $R_0$, $R_1$, $R_2$, $C_1$ and $C_2$ with SOC, which is regarded as the input value of the second-order RC battery model to get the analog voltage value and then compared with the actual voltage value to discuss the precision of online parameter identification. The analysis of the validation results is shown in Fig. 6.

According to Fig. 6(b), in each discharge cycle, the simulation voltage error is relatively large at the moment of sudden change of current, which is related to the violent chemical reaction inside the lithium-ion battery. The maximum error of the simulation voltage is -0.0390V, controlled within 0.92%, which can be applied to the next SOC estimation with high accuracy.

### *3.3. Experimental verification under HPPC operating condition*

To verify the feasibility of the proposed algorithm, the HPPC experimental data and online battery parameter identification results are used for SOC estimation firstly, the initial SOC value of is set to 1. The simulation results of basic PF and IWDF - PF under HPPC operating condition are shown in Fig. 7.

According to Fig. 7 (b), obviously, the overall accuracy of IWDF - PF is higher, the real value can be tracked better in the whole discharge process, and the fluctuation is small. In contrast, the error of PF fluctuates greatly, while IWDF - PF solves the problem of easy divergence in the later stage of traditional PF. The experimental results of the two algorithms are compared through the maximum error, mean absolute error (MAE) and root-mean-square error (RMSE) under HPPC test as shown in Tab. 1.

### *3.4. Experimental verification under BBDST operating condition*

The actual operating conditions of lithium-ion batteries for vehicles are very changeable and complex, it is certainly need to verify the proposed algorithm with more real and dynamic data. BBDST test data is obtained from the real data collection of Beijing bus dynamic stress test, including the current and voltage data in the complete operation process of bus operation, such as starting, acceleration, taxiing, braking, rapid acceleration and parking, which has strong authenticity and dynamics. The simulation results of basic PF and IWDF - PF under BBDST test when the initial SOC value is set to 1 are shown in Fig. 8.

According to Fig. 8(b), the error of PF algorithm fluctuates greatly, and the accuracy in the later stage is extremely unstable and the divergence degree is high. Obviously, the error of IWDF - PF algorithm is very stable, the estimated value always tracks the real value well, and the error is always controlled within a reasonable range. The maximum error of PF is as high as 4.89%, while it of IWDF - PF is only 2.37%.

To verify the robustness of the proposed algorithm, SOC is given different initial values for verification. The simulation results of basic PF and IWDF - PF under BBDST test when the initial SOC value of is set to 0.9 are shown in Fig. 9.

As can be seen from Fig. 9(b), even if the SOC initial value with high interference is set, the algorithm still has good convergence and high precision. The error of IWDF - PF algorithm in the whole discharge cycle is obviously smaller than that of the traditional algorithm, and the problem of easy divergence in the later stage is solved. It can be seen that the firefly algorithm with decreasing weight has a very considerable improvement on the traditional PF, which also has strong anti-interference ability. The experimental results of the two algorithms under different initial SOC value settings are compared through the maximum error, MAE and RMSE under BBDST working condition as shown in Tab. 2.

## 4. Conclusions

Accurate real-time status supervision of power vehicle lithium-ion batteries is extremely important. In this paper, based on the second-order RC equivalent modeling and online parameter identification, the firefly algorithm is introduced to complete the optimization process of state-of-charge particles by simulating the mutual attraction behavior of fireflies in nature, to break this dilemma of particle degradation. The weight decreasing strategy is added to improve the convergence speed of firefly algorithm. The conclusions of this research can be summarized as follows:

(1) The state-of-charge estimation results when the initial value is set to 1 show that the root-mean-square error of the novel intelligent weight decreasing firefly - particle filtering method under Hybrid Pulse Power Characterization and Beijing Bus Dynamic Stress Test condition can be controlled within 0.60% and 1.12% respectively, the accuracy of the improved algorithm is improved by 0.59% and 1.38% respectively, which proves the progressiveness and effectiveness of the proposed algorithm.

(2) The robustness of the algorithm is verified by setting different initial values for SOC. The state-of-charge estimation results when the initial value is set to 0.9 show that the root-mean-square error of the novel intelligent weight decreasing firefly - particle filtering method under Beijing Bus Dynamic Stress Test condition can be controlled within 1.22%, the accuracy of the improved algorithm is improved by 1.94%, which proves that the proposed algorithm still has good adjustment and adaptive ability for the initial value setting with great inaccuracy, and can still maintain high accuracy in the face of abnormal conditions. Therefore, the proposed algorithm has good robustness.

In conclusion, the proposed algorithm is feasible to improve the state-of-charge estimation accuracy of lithium-ion batteries. This research provides a theoretical foundation for real-time state monitoring and safe operation of new energy vehicles in practical application.

## Acknowledgments

The work is supported by the National Natural Science Foundation of China (No. 62173281, 61801407), Sichuan science and technology program (No. 2019YFG0427), China Scholarship Council (No. 201908515099), and Fund of Robot Technology Used for Special Environment Key Laboratory of Sichuan Province (No. 18kftk03).

## References

1. Chen, L., et al., *Decreasing Weight Particle Swarm Optimization Combined with Unscented Particle Filter for the Non-Linear Model for Lithium Battery State of Charge Estimation.* International Journal of Electrochemical Science,

2020. **15**(10): p. 10104-10116.

2. Meng, J.H., et al., *An optimized ensemble learning framework for lithium-ion Battery State of Health estimation in energy storage system.* Energy, 2021. **206**: p. 1-16.
3. Hu, X.S., et al., *Battery Health Prediction Using Fusion-Based Feature Selection and Machine Learning.* Ieee Transactions on Transportation Electrification, 2021. **7**(2): p. 382-398.
4. Hu, X.S., et al., *A Control-Oriented Electrothermal Model for Pouch-Type Electric Vehicle Batteries.* Ieee Transactions on Power Electronics, 2021. **36**(5): p. 5530-5544.
5. Wang, Y. and Z. Chen, *A framework for state-of-charge and remaining discharge time prediction using unscented particle filter.* Applied Energy, 2020. **260**: p. 1-15.
6. Wang, Y.J., et al., *A comprehensive review of battery modeling and state estimation approaches for advanced battery management systems.* Renewable & Sustainable Energy Reviews, 2020. **131**: p. 1-14.
7. Xu, W., J. Xu, and X. Yan, *Lithium-ion battery state of charge and parameters joint estimation using cubature Kalman filter and particle filter.* Journal of Power Electronics, 2020. **20**(1): p. 292-307.
8. Al-Gabalawy, M., et al., *State of charge estimation of a Li-ion battery based on extended Kalman filtering and sensor bias.* International Journal of Energy Research, 2021. **45**(5): p. 6708-6726.
9. Chen, Y., et al., *A combined robust approach based on auto-regressive long short-term memory network and moving horizon estimation for state-of-charge estimation of lithium-ion batteries.* International Journal of Energy Research, 2021. **45**(9): p. 12838-12853.
10. Li, J., et al., *Joint estimation of state of charge and state of health for lithium-ion battery based on dual adaptive extended Kalman filter.* International Journal of Energy Research, 2021. **45**(9): p. 13307-13322.
11. Chen, Z.H., et al., *Particle filter-based state-of-charge estimation and remaining-dischargeable-time prediction method for lithium-ion batteries.* Journal of Power Sources, 2019. **414**: p. 158-166.
12. Beelen, H., H.J. Bergveld, and M.C.F. Donkers, *Joint Estimation of Battery Parameters and State of Charge Using an Extended Kalman Filter: A Single-Parameter Tuning Approach.* Ieee Transactions on Control Systems Technology, 2021. **29**(3): p. 1087-1101.
13. Meng, J.H., et al., *A Simplified Mode Based State-of-Charge Estimation Approach for Lithium-Ion Battery With Dynamic Linear Model.* Ieee Transactions on Industrial Electronics, 2019. **66**(10): p. 7717-7727.
14. Gholizadeh, M. and A. Yazdizadeh, *Systematic mixed adaptive observer and EKF approach to estimate SOC and SOH of lithium-ion battery.* Iet Electrical Systems in Transportation, 2020. **10**(2): p. 135-143.
15. Huang, Z., Y. Fang, and J. Xu, *SOC ESTIMATION OF Li-ION BATTERY BASED ON IMPROVED EKF ALGORITHM.* International Journal of Automotive Technology, 2021. **22**(2): p. 335-340.
16. Li, W., et al., *The multi-innovation extended Kalman filter algorithm for battery SOC estimation.* Ionics, 2020. **26**(12): p. 6145-6156.
17. Zhang, K., et al., *State of Charge Estimation for Lithium Battery Based on Adaptively Weighting Cubature Particle Filter.* IEEE ACCESS, 2019. **7**: p. 166657-166666.
18. Shi, H., et al., *A novel dual correction extended Kalman filtering algorithm for the state of charge real-time estimation of packing lithium-ion batteries*. International Journal of Electrochemical Science, 2021. **15**: p. 12706-12723.
19. Shi, H., et al., *Improved splice-electrochemical circuit polarization modeling and optimized dynamic functional multi-innovation least square parameter identification for lithium-ion batteries.* International Journal of Energy Research, 2021. **45**(10): p. 15323-15337.
20. Ren, P., et al., *Novel co-estimation strategy based on forgetting factor dual particle filter algorithm for the state of charge and state of health of the lithium-ion battery.* International Journal of Energy Research, 2021. **45**(10): p. 1-15.
21. Miao, H., et al., *A novel online model parameters identification method with anti-interference characteristics for lithium-ion batteries.* International Journal of Energy Research, 2021. **45**(6): p. 9502-9517.

22. Xu, W., et al., *A novel adaptive dual extended Kalman filtering algorithm for the Li-ion battery state of charge and state of health co-estimation.* International Journal of Energy Research, 2021. **45**(10): p. 14592-14602.
23. Xiong, X., et al., *A novel practical state of charge estimation method: an adaptive improved ampere-hour method based on composite correction factor.* International Journal of Energy Research, 2020. **44**(14): p. 11385-11404.
24. Meng, J., et al., *An Overview and Comparison of Online Implementable SOC Estimation Methods for Lithium-Ion Battery.* Ieee Transactions on Industry Applications, 2018. **54**(2): p. 1583-1591.
25. Li, Y., et al., *Comparative Study of the Influence of Open Circuit Voltage Tests on State of Charge Online Estimation for Lithium-Ion Batteries.* Ieee Access, 2020. **8**: p. 17535-17547.
26. Liu, Y., et al., *State of Charge Estimation for Li-Ion Batteries Based on an Unscented H-Infinity Filter.* Journal of Electrical Engineering & Technology, 2020. **15**(6): p. 2529-2538.
27. Xiong, R., et al., *A set membership theory based parameter and state of charge co-estimation method for all-climate batteries.* Journal of Cleaner Production, 2020. **249**: p. 1-14.
28. Ouyang, Q., J. Chen, and J. Zheng, *State-of-Charge Observer Design for Batteries With Online Model Parameter Identification: A Robust Approach.* Ieee Transactions on Power Electronics, 2020. **35**(6): p. 5820-5831.
29. Zhang, S. and J. Zhang, *Optimal State-of-Charge Value for Charge-Sustaining Mode of Plug-In Hybrid Electric Vehicles.* Ieee Access, 2020. **8**: p. 187959-187964.
30. Chen, Y., et al., *Remaining Useful Life Prediction and State of Health Diagnosis of Lithium-Ion Battery Based on Second-Order Central Difference Particle Filter.* Ieee Access, 2020. **8**: p. 37305-37313.
31. Wang, K., et al., *An Improved SOC Control Strategy for Electric Vehicle Hybrid Energy Storage Systems.* Energies, 2020. **13**(20) : p. 1-13.

Tab. 1 Comparison of SOC estimation results under HPPC test

| Estimation method | PF | IWDF - PF |
|---|---|---|
| Maximum Error | 2.29% | 1.39% |
| MAE | 1.04% | 0.48% |
| RMSE | 1.19% | 0.60% |

Tab. 2 Comparison of SOC estimation results under BBDST test

| Estimation method | PF | IWDF - PF |
|---|---|---|
| Maximum Error (Initial SOC = 1) | 4.89% | 2.37% |
| MAE (Initial SOC = 1) | 2.19% | 0.96% |
| RMSE (Initial SOC = 1) | 2.50% | 1.12% |
| Maximum Error (Initial SOC = 0.9) | 6.01% | 1.83% |
| MAE (Initial SOC = 0.9) | 2.99% | 1.09% |
| RMSE (Initial SOC = 0.9) | 3.16% | 1.22% |

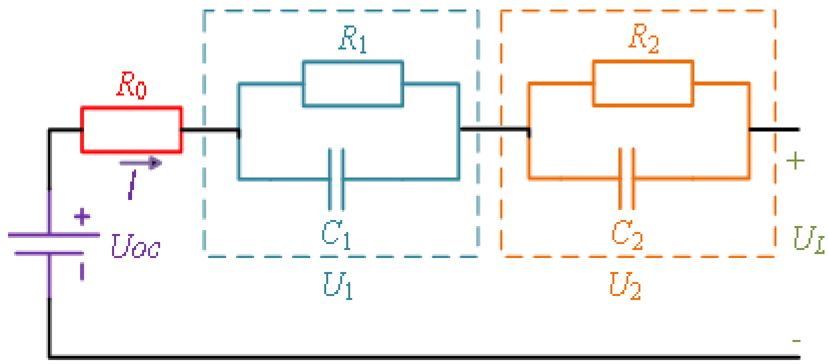


Second-order RC equivalent circuit model

87x53mm (120 x 120 DPI)

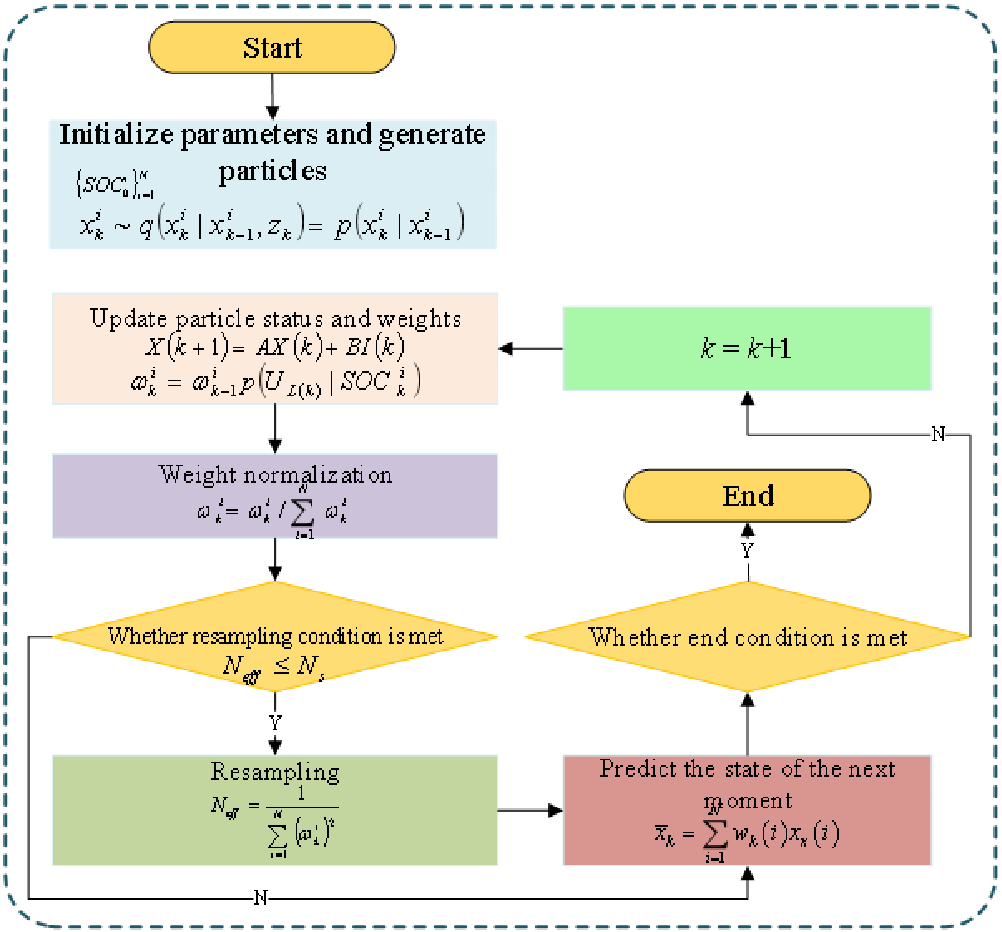


Process of basic PF algorithm

127x118mm (120 x 120 DPI)

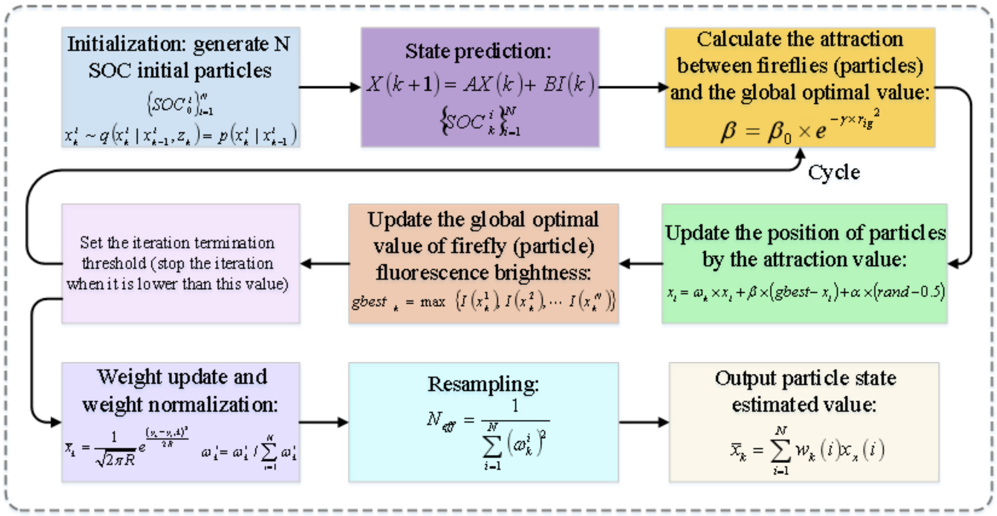


Complete process of the proposed novel IWDF - PF method

175x90mm (120 x 120 DPI)

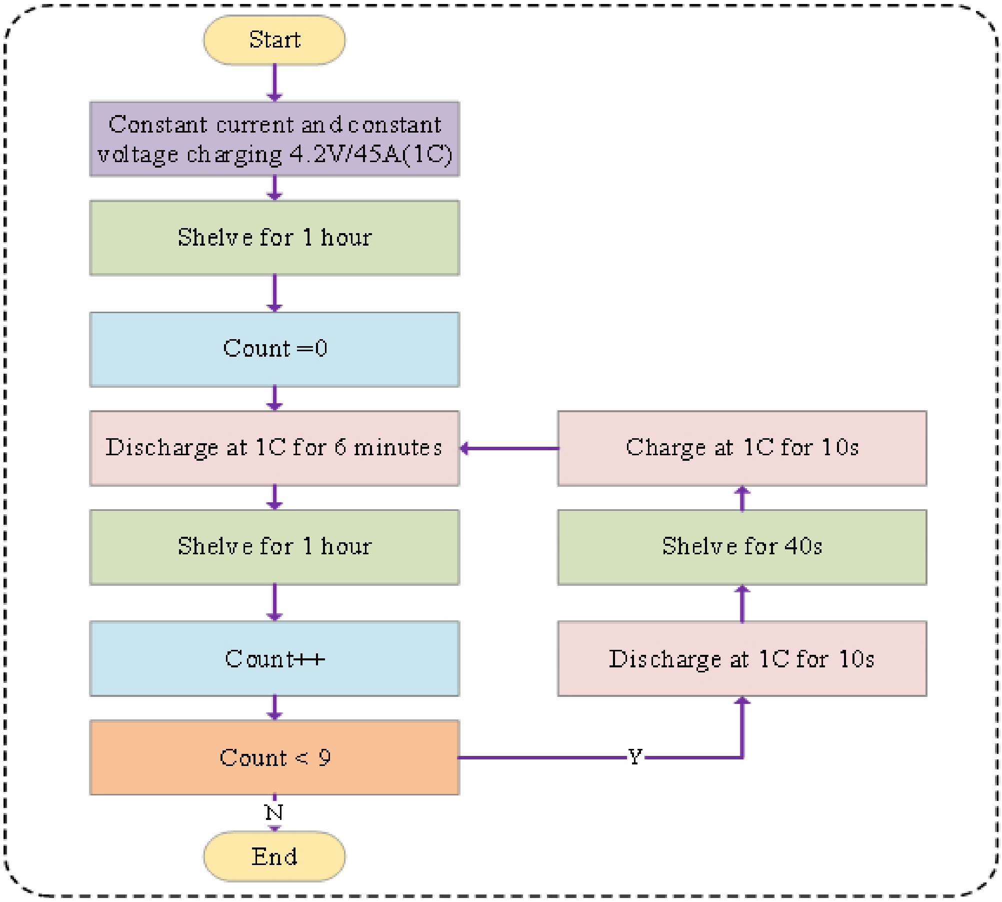


Whole process of HPPC experiment

121x109mm (120 x 120 DPI)

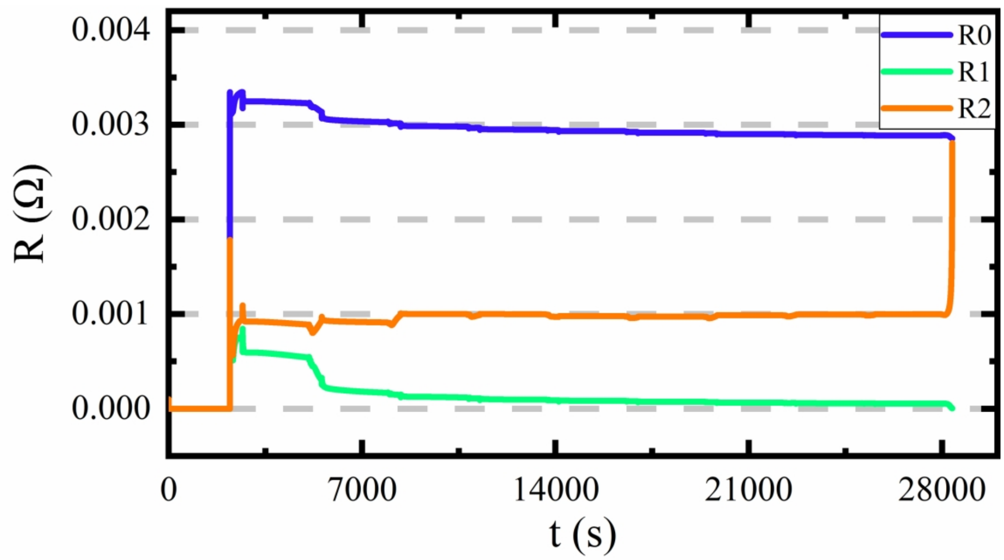


Dynamic changes of R0, R1 and R2 with SOC

179x99mm (300 x 300 DPI)

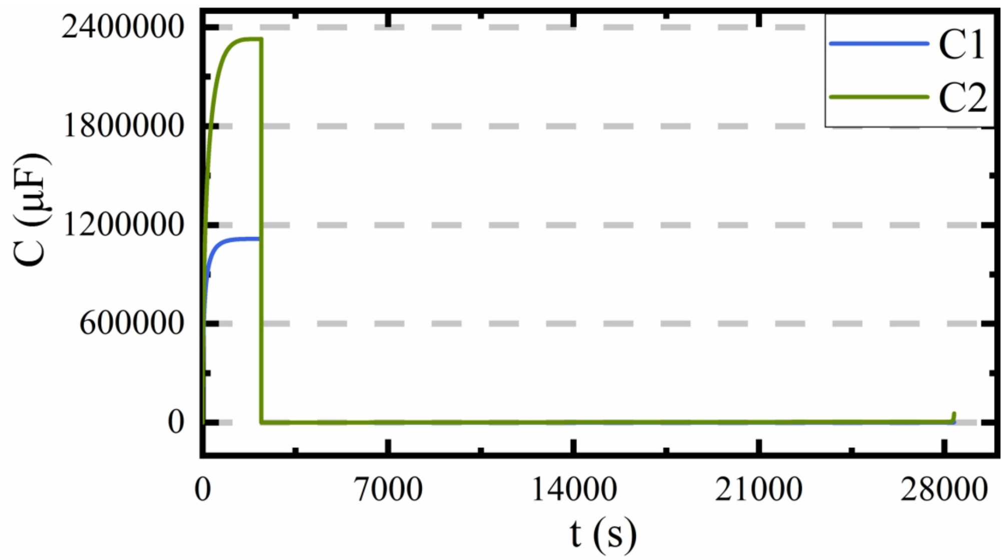


Dynamic changes of C1 and C2 with SOC

179x99mm (300 x 300 DPI)

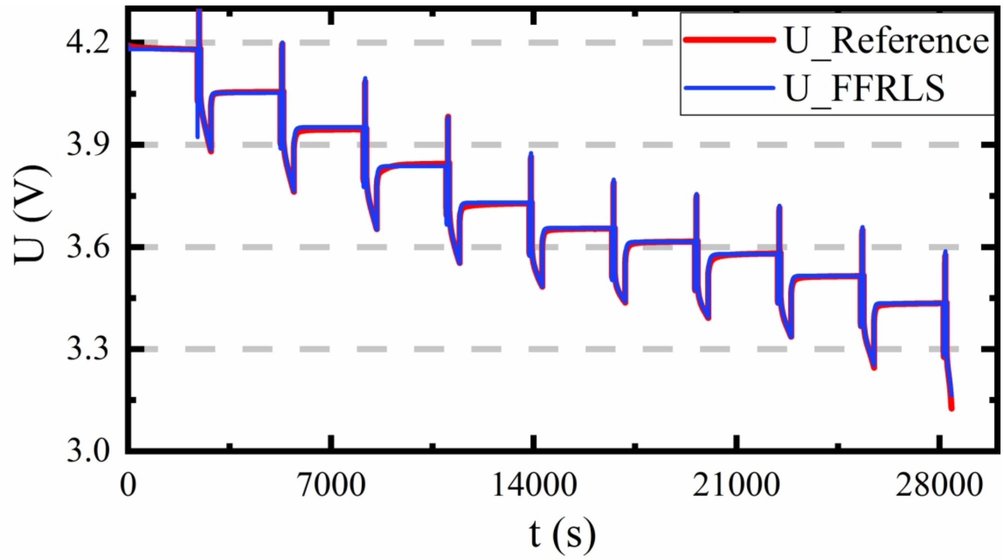


Comparison between simulated voltage and actual voltage under HPPC test

179x99mm (300 x 300 DPI)

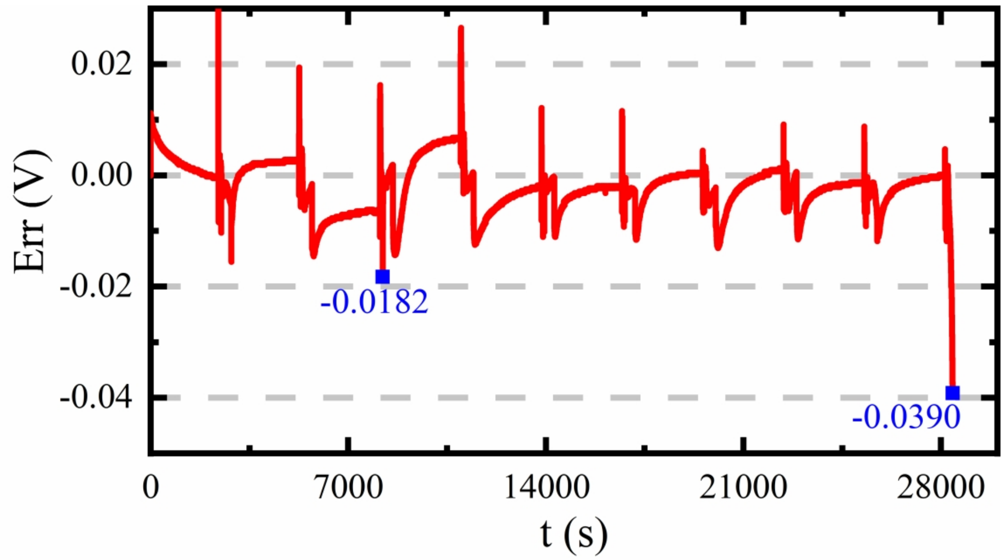


Voltage error under HPPC test

179x99mm (600 x 600 DPI)

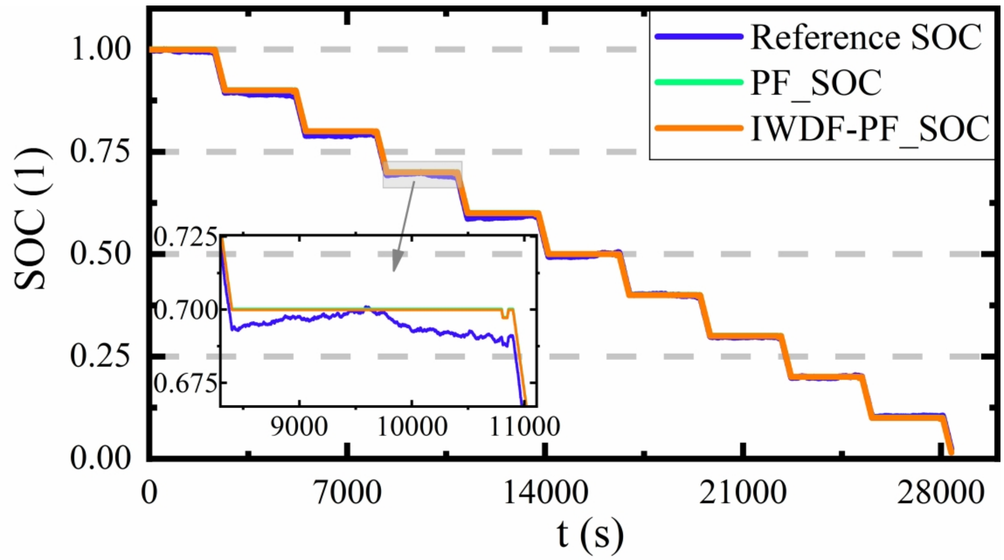


SOC estimation results under HPPC test when SOC initial value is 1

179x99mm (600 x 600 DPI)

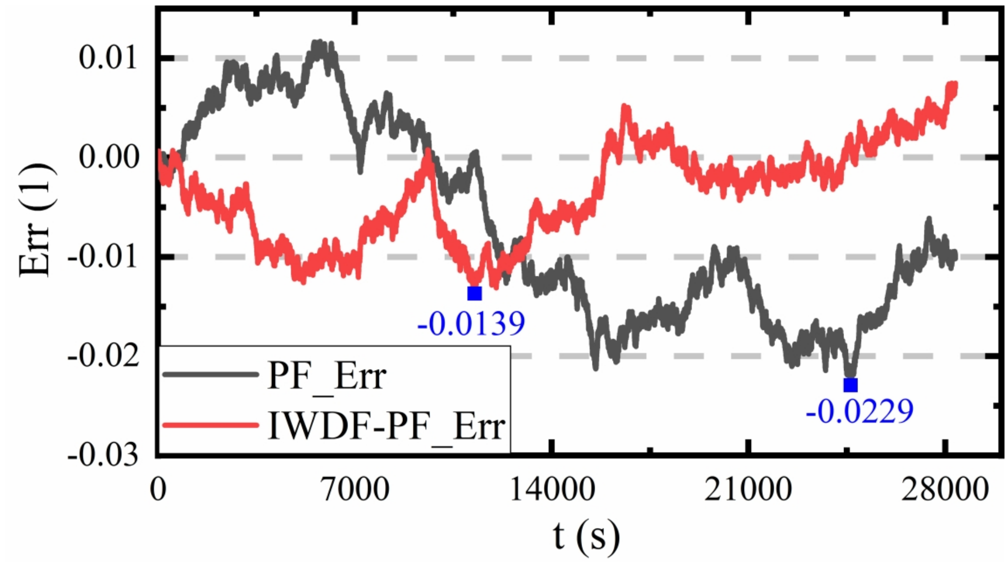


SOC estimation error under HPPC test when SOC initial value is 1

179x99mm (600 x 600 DPI)

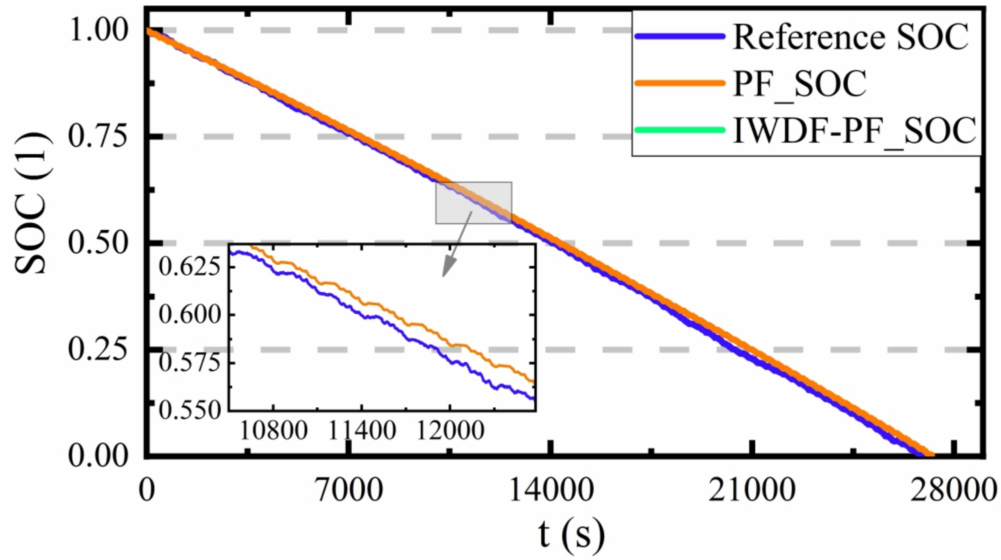


SOC estimation results under BBDST test when SOC initial value is 1

180x99mm (600 x 600 DPI)

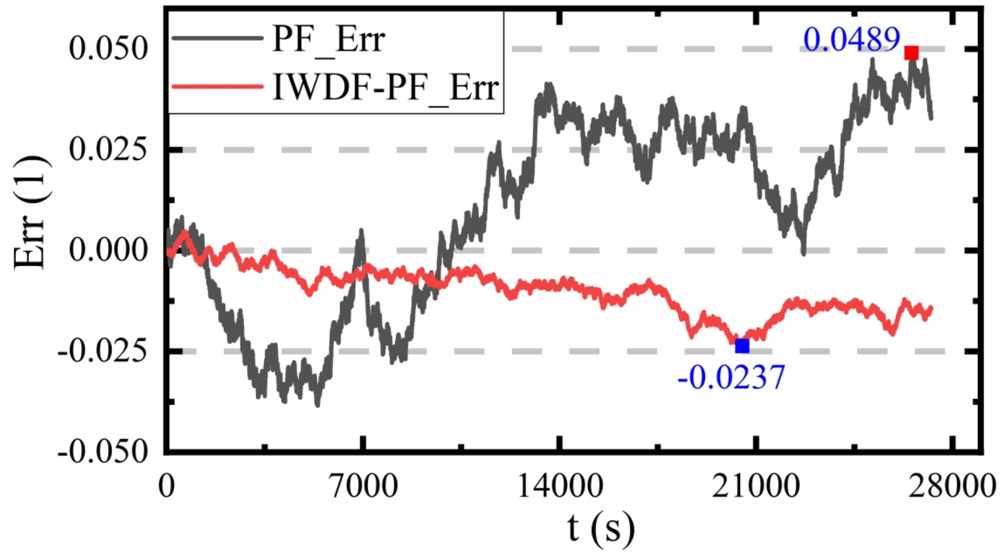


SOC estimation error under BBDST test when SOC initial value is 1

178x98mm (600 x 600 DPI)

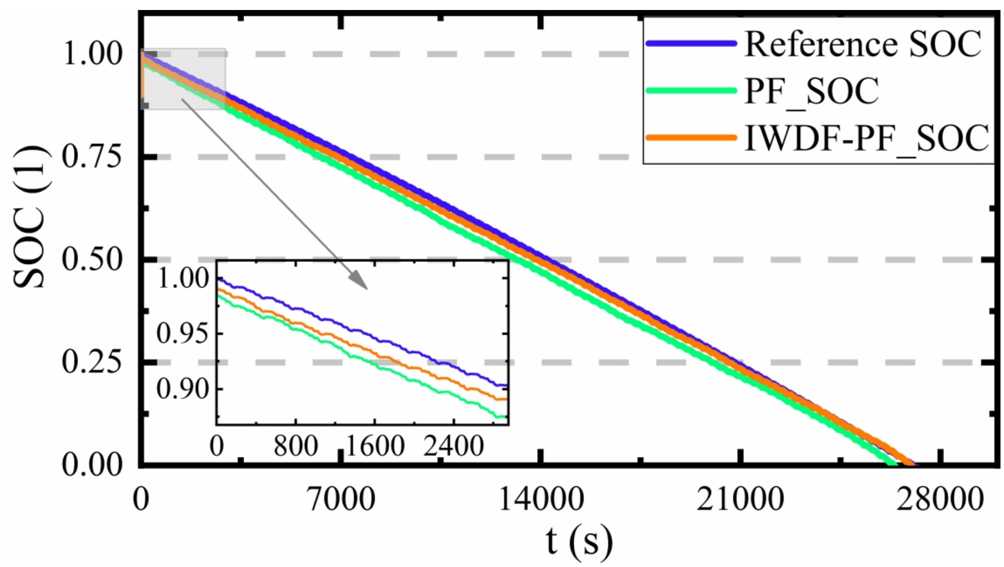


SOC estimation results under BBDST test when SOC initial value is 0.9

179x99mm (600 x 600 DPI)

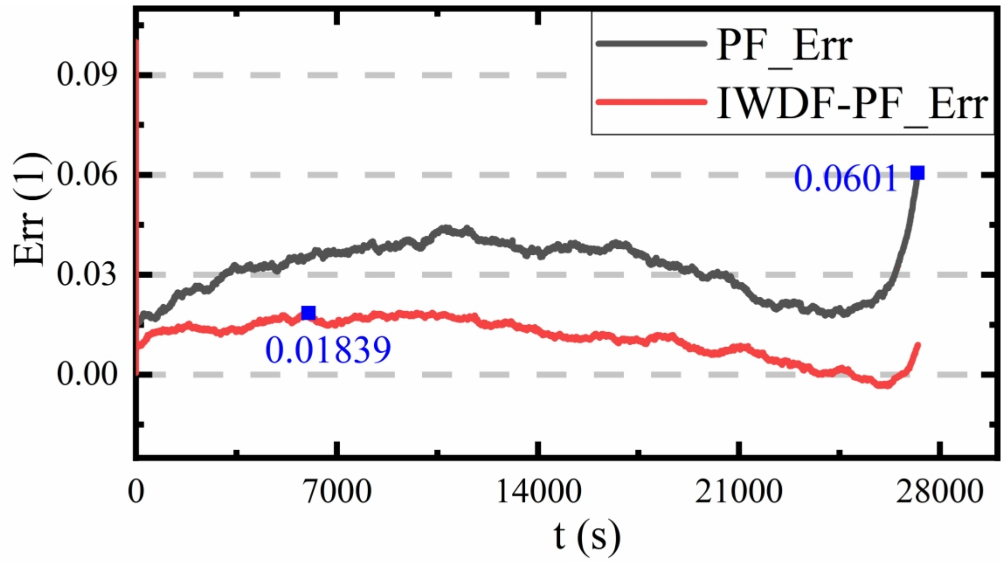


SOC estimation error under BBDST test when SOC initial value is 0.9

179x99mm (600 x 600 DPI)